DOI: 10.1002/cbic.200800556

Differential Effects of Natural Product Microtubule Stabilizers on Microtubule Assembly: Single Agent and Combination Studies with Taxol, Epothilone B, and Discodermolide

Jürg Gertsch,[a] Sarah Meier,[a] Martin Müller,[b] and Karl-Heinz Altmann*[a]

A systematic comparison has been performed of the morphology and stability of microtubules (MTs) induced by the potent microtubule-stabilizing agents (MSAs) taxol, epothilone B (Epo B), and discodermolide (DDM) under GTP-free conditions. DDM-induced tubulin polymerization occurred significantly faster than that induced by taxol and Epo B. At the same time, tubulin polymers assembled from soluble tubulin by DDM were morphologically distinct (shorter and less ordered) from those induced by either taxol or Epo B, as demonstrated by electron microscopy. Exposure of MSA-induced tubulin polymers to ultrasound revealed the DDM-based polymers to be less stable to this type of physical stress than those formed with either Epo B or taxol. Interestingly, MT assembly in the presence of both DDM and taxol appeared to produce a distinct new type of MT polymer with a mixed morphology between those of DDM- and taxol-induced structures. The observed differences in MT morphology and stability might be related, at least partly, to differences in intramicrotubular tubulin isotype distribution, as DDM showed a different pattern of β-tubulin isotype usage in the assembly process.

Introduction

Taxol, epothilone B (Epo B), and discodermolide (DDM) all belong to a larger group of structurally diverse natural products, whose common characteristic is their ability to stabilize cellular microtubules (MTs) and to promote the polymerization of soluble tubulin.[1]

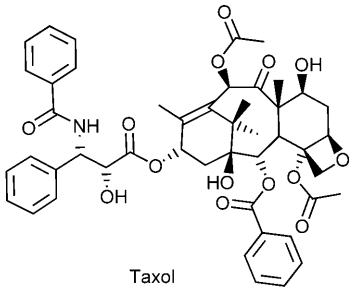

Taxol

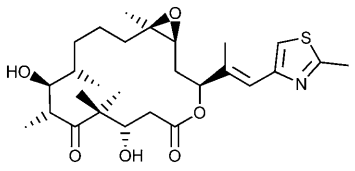

Epothilone B (Epo B)

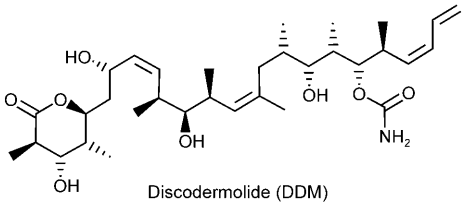

Discodermolide (DDM)

MTs are rod-shaped hollow filaments composed of the heterodimeric protein $\alpha\beta$-tubulin as the constituent subunit.[2] They are key components of the cytoskeleton of eukaryotic cells, where they are involved in the spatial distribution of organelles throughout interphase and in chromosome alignment and sister chromatide separation during mitosis. As a consequence, the interference with MT functionality by MT-stabilizing agents (MSAs) is associated with cell cycle arrest at G_2/M, profound growth inhibition, and the induction of apoptosis.[1,2a] However, it is important to note that growth inhibition and apoptosis induction by MSAs in general do not depend on gross changes in the cellular equilibrium between soluble and polymerized tubulin. Rather, these effects might be caused by alterations in MT dynamics,[2a,3] that is, the continuous change in MT length through the loss or addition of $\alpha\beta$-tubulin units at polymer ends. The dynamic properties of MTs are a crucial requirement in the proper assembly of the mitotic spindle and the subsequent movement of sister chromatids to the spindle

[a] *Dr. J. Gertsch, S. Meier, Prof. Dr. K.-H. Altmann*
Swiss Federal Institute of Technology (ETH) Zürich
Department of Chemistry and Applied Biosciences
Institute of Pharmaceutical Sciences, HCI H405
Wolfgang-Pauli-Strasse 10, 8093 Zürich (Switzerland)
Fax: (+41) 44-6331360
E-mail: karl-heinz.altmann@pharma.ethz.ch

[b] *Dr. M. Müller*
Swiss Federal Institute of Technology (ETH) Zürich
Department of Physics, 8093 Zürich (Switzerland)

poles, with spindle MTs being up to 100-fold more dynamic than those forming the interphase cytoskeleton.[4] In light of their profound inhibition of human cancer cell growth, it is no surprise that MSAs play an important role in cancer chemotherapy and anticancer drug discovery, with taxol (paclitaxel, Taxol®) and its closely related analogue docetaxel (Taxotere®) being two of the most important anticancer drugs currently in use.[5] Taxol was the first MT stabilizer ever discovered[6] (with its mechanism of action elucidated in 1979[7]) and was first approved for clinical use in 1992. Epo B[8] and DDM are still experimental agents, but both compounds have entered clinical trials in humans,[9,10] and Epo B is currently undergoing phase III studies against ovarian cancer.[11] The lactam analogue of Epo B (BMS-247550, ixabepilone) was approved by the US FDA for the treatment of metastatic and advanced breast cancer in October 2007.[12]

In contrast to taxol, both Epo B[13] and DDM[14] are poor substrates for the p-gp170 efflux pump, and as a consequence, retain potent in vitro antiproliferative activity against a variety of taxol-resistant human cancer cell lines. Perhaps the most intriguing finding in the context of human cancer cell growth inhibition by taxol, Epo B, and DDM, however, is the fact that combinations of DDM and taxol exhibit synergistic antiproliferative effects both in vitro[14a] and in vivo,[15] whereas no synergy occurs between DDM and Epo B or taxol and Epo B. The synergistic inhibition of human cancer cell growth by DDM and taxol is paralleled by a corresponding synergistic suppression of cellular MT dynamics,[16] thus providing a possible mechanistic rationale for the intriguing combination effects at the level of growth inhibition.

As demonstrated by competition binding experiments, taxol, Epo B, and DDM all bind to the same site on β-tubulin, albeit with different affinities.[17] Likewise, the three compounds promote MT assembly from soluble tubulin with distinctly different efficiencies. Based on the critical tubulin concentration, $[T]_{cr}$ (i.e., the minimum concentration of tubulin required for the initiation of polymer formation), as a measure of polymerizing potency, DDM is a more potent inducer of tubulin polymerization than Epo B, and both are significantly more potent than taxol.[17] For all three compounds, the polymers formed under appropriate conditions were demonstrated to be MTs by electron microscopy (EM);[1a] however, DDM-induced MTs were significantly shorter than those obtained with taxol or Epo B[18] (e.g., MT lengths of 0.78 and 3.3 μm were reported for DDM and taxol, respectively, under identical experimental conditions[18a]), and DDM-based polymer preparations were also reported to contain a significant fraction of ribbon polymers (as opposed to cylindrical MTs).[18b] These latter data clearly point to the dependence of gross MT architecture on the specific polymerizing agent, even for compounds interacting with the same tubulin-binding site. In spite of this fact, however, the morphology of MSA-induced MTs as a function of the polymerizing agent, or, in particular, combinations of different agents, has not been investigated in great detail. Notable exceptions are the work of Meurer-Grob et al.,[19] who have shown that MTs assembled by a series of different MSAs (not including DDM) might incorporate different numbers of protofilaments, and a more recent study by Hamel and co-workers,[20] who investigated the effects of combinations of laulimalide with taxol or epothilone A, respectively, on tubulin polymerization induction, MT stability, and gross MT architecture. It should be noted, however, that laulimalide does not bind to the taxol site on β-tubulin.[17,21,22]

In this study, we have performed a systematic comparison of the morphology and stability of MTs induced by taxol, Epo B, and DDM from purified pig brain tubulin under GTP-free conditions using turbidity measurements, ultrasound (US) treatment, structural analysis by EM, and semiquantitative β-isoform analysis. In particular, this has included the assessment of combination effects for all three binary combinations of these agents, as it is well conceivable that the synergism between DDM and taxol in the suppression of cellular MT dynamics and the associated inhibition of cancer cell growth might originate from, or at least be connected to, effects on MT architecture.

Results and Discussion

Tubulin polymerization

The induction of tubulin polymerization by the MSAs taxol, Epo B, and DDM in the absence of both glutamate and GTP was assessed either by turbidimetry analysis (following the increase in absorbance at 340 nm (ΔA_{340}) upon polymer formation)[23] or in a centrifugation-based assay, which involved the quantification of unpolymerized soluble tubulin in the supernatant of centrifuged polymerization mixtures.[24] With both methods, maximum tubulin polymerization was observed at equimolar MSA/tubulin ratios for all three compounds; no further increase in the degree of polymer formation was detectable with compound concentrations in excess of that of tubulin (data not shown; these findings are in line with previous literature observations for all three agents[25,26]). However, significant differences occurred between taxol, Epo B, and DDM with respect to the time period, T_{max}, required to achieve maximum tubulin polymerization under identical experimental conditions (Mg^{2+}, no glutamate or GTP). Thus, the T_{max} for DDM in the centrifugation-based polymerization assay, as defined as the time elapsed after initiation of the polymerization reaction until no further decrease in the amount of soluble tubulin could be detected, was (420 ± 139) s, which was significantly smaller than the values obtained for taxol, (1024 ± 177) s, and Epo B, (1530 ± 281) s. This indicated a much more rapid completion of the polymerization reaction for DDM than for taxol or Epo B. To further support this conclusion, attempts were made to derive T_{max} values from the polymerization-associated changes at A_{340}. However, the determination of T_{max} in the turbidimetry-based assay was complicated by the fact that the concentrations of soluble tubulin in the polymerization mixtures (as determined by the centrifugation method) continued to decrease even after a plateau in the absorption curve had been reached. This indicated that equilibrium was not achieved even when the absorption of the polymerization mixture ceased to change. An alternative method was thus developed for the assessment of T_{max} by means of turbidimetry measure-

ments, which involved the addition of GTP to MSA-containing polymerization mixtures at different times after the initiation of polymerization. In the presence of soluble, polymerizable tubulin, the addition of GTP was assumed to give rise to a "second polymerization curve" (a separate discrete increase in absorption). This was indeed observed (Figure 1 A and B), and T_{max} was defined as the time point when the addition of GTP failed to trigger any further increase in A_{340}. Using this approach, T_{max} values of (1490 ± 411) s and (1711 ± 462) s could be determined for taxol and Epo B, respectively; these numbers agreed reasonably well with those obtained in the centrifugation-based assay.

Unfortunately, no sensible T_{max} could be determined for DDM by the turbidimetry method, due to the fact that the addition of GTP to DDM-containing polymerization mixtures led to a dramatic second increase in A_{340} (>40%) even long after the centrifugation-based T_{max} had been reached (Figure 1 C). While the reasons for this phenomenon are unclear at this point and need to be elucidated in further experiments, it should be noted that the strong increase in the A_{340} observed upon the addition of GTP to DDM-containing polymerization mixtures after 30 min of (GTP-free) incubation cannot be explained by the existence of large amounts of residual soluble tubulin that would undergo polymerization only with GTP, but not with DDM, which was our original hypothesis. Only small differences were found for the maximum degree of conversion of tubulin into MT polymers between taxol (88%), Epo B (91%) and DDM (89%; in the absence of glutamate and GTP) and DDM + GTP (92%; addition of GTP once an absorption plateau had been reached with with DDM alone, Figure 1 C).

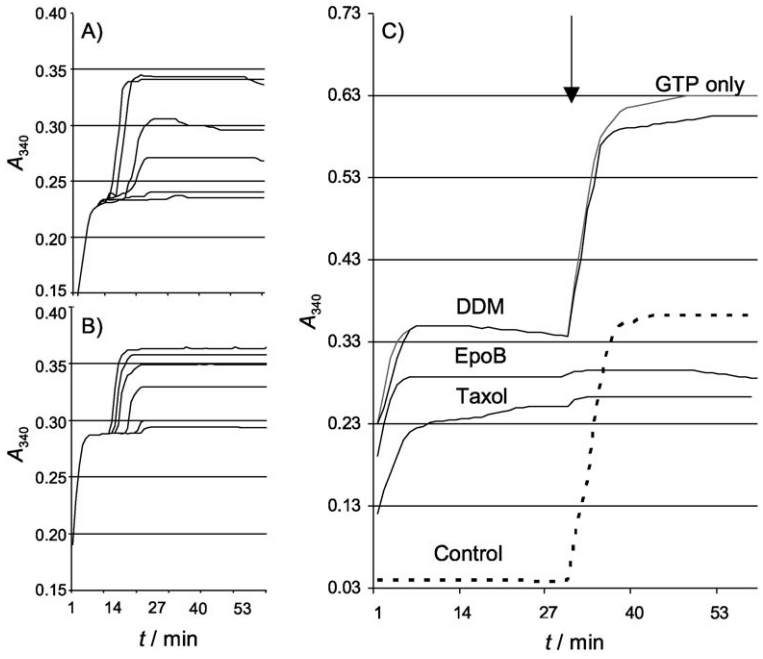

Figure 1. A) Determination of T_{max} by turbidimetry. αβ-Tubulin (50 μM) was treated with Epo B (50 μM) at room temperature. GTP (25 mM) and glutamate (2.7 M) were added at different time points after a first plateau (A_{340}) was reached. The T_{max} was calculated from Graphpad Prism 4 curve fitting as the time point at which no further increase in A_{340} was detected. B) Same experiment as for A), but with taxol. C) Effect of GTP addition to DDM-, taxol-, or Epo B-containing tubulin polymerization mixtures. αβ-Tubulin (50 μM) was treated with MSA (50 μM) at room temperature for 30 min prior to the addition of GTP (25 mM) and glutamate (2.7 M). The addition of GTP and glutamate (↓) leads to a marked second polymerization curve with DDM-induced MTs, but not with taxol- or Epo B-containing MT samples. The unpolymerized fraction in the DDM-treated sample can be assembled by GTP alone without glutamate (gray curve). A tubulin only (no MSA) negative control is shown (····).

MT size and morphology

In order to expand on the results obtained in the polymerization assays, EM was employed for a semiquantitative assessment of the number and size of MTs produced with taxol, Epo B, and DDM under our experimental conditions (in BBR80 buffer containing 1 mM $MgCl_2$ and no glutamate or GTP; for the composition of BBR80 buffer see the Experimental Section).

The corresponding micrographs clearly showed that taxol and Epo B led to the formation of few but relatively long (1–10 μm) MTs (Figure 2). In contrast, DDM-induced MTs were short (~1 μm), but the number of MTs formed was significantly greater than that for either taxol ($P = 0.0005$) or Epo B ($P = 0.0003$; pictures not shown). Similar size characteristics for DDM-induced MTs have been reported previously for different experimental conditions.[18]

A closer inspection of the polymeric structures formed in the presence of the three different MSAs revealed a number of major architectural differences between the polymers formed with DDM on one hand and those induced by either taxol or Epo B on the other (apart from the difference in size). While taxol and Epo B formed regular and straight MTs in our system (Figure 2 B–D), DDM-induced tubulin polymers were typically twisted and frayed and there were numerous ribbons and sheets visible in the electron micrographs (Figures 2 A, E, and 3). In general, more than 50% of the DDM-polymerized tubulin was present in sheets.

The presence of ribbon-type structures in DDM-induced tubulin polymers was observed previously by Hamel and coworkers.[18b] In their experiments, the fraction of ribbons was largest under conditions with only GTP in the polymerization mixture, while mostly regular MTs formed in the absence of GTP and MT-associated proteins (MAPs), which were the conditions employed here. These discrepancies may be due to differences in other experimental parameters that cannot be traced. Most importantly, however, no further analysis of DDM-induced polymers was performed in Hamel's study.

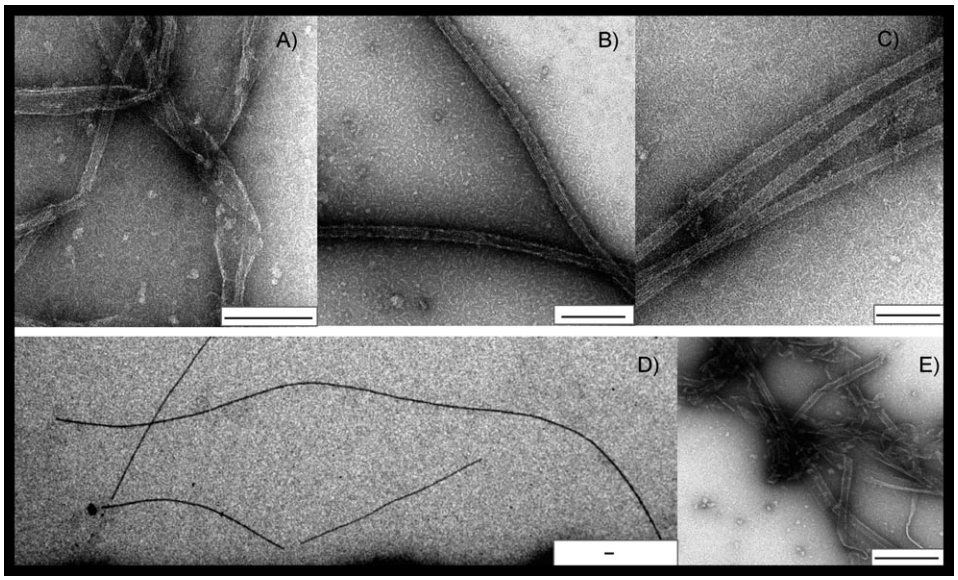

Figure 2. Electron micrographs of MTs induced by equimolar amounts of different MSAs at 40 μM αβ-tubulin concentration. A) DDM-induced MT fragments. B) Taxol-induced MTs. C) Epo B-induced MTs. D) Electron micrograph showing long (>13 μm) MTs induced by Epo B. E) Tubulin polymers induced by DDM in the presence of MAPs (0.5 mg mL^{-1}). The size of the scale bar is 200 nm in all cases. All polymers were formed in the absence of GTP (see the Experimental Section).

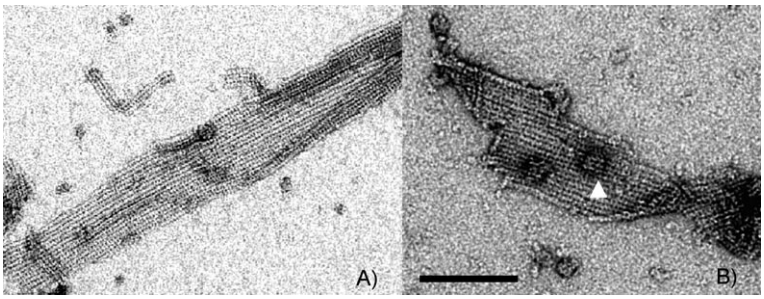

Figure 3. A) DDM-induced αβ-tubulin sheet composed of 18 protofilaments. The longitudinal and lateral contacts are broken. B) A typical αβ-tubulin sheet induced by DDM. At its maximum width, the sheet is composed of 20 protofilaments. Also visible are convoluted protofilaments that appear as globular particles (white arrow head). Polymerization was induced by equimolar amounts of DDM at 20 μM αβ-tubulin concentration. The size of the scale bar is 30 nm.

In order to assess the number of protofilaments in DDM-induced MT polymers (at 40 μM MSA/tubulin), 40 cylindrical MTs from two independent experiments were analyzed and >90% of these polymers were found to be composed of 10–14 protofilaments. (In general, MTs assembled in vitro incorporate between 12 and 14 protofilaments[2d]). In contrast, DDM-induced tubulin sheets contained up to 22 protofilaments (Figure 3). The formation of polymeric sheets could occur either through the opening of MT cylinders or by the lateral assembly of protofilaments, which do not close to form a cylinder. The existing data do not allow us to distinguish between these possibilities, but given the large number of protofilaments in the sheets (>18), the direct lateral assembly of protofilaments may be the more likely mechanism of sheet formation.

Excess drug concentrations, relative to that of tubulin, showed a tendency to increase the fraction of sheets in the overall polymer population. In this context, it is worth noting that the increase in adsorption (ΔA_{340}) observed in the turbidimetry experiments with DDM has to be assumed to reflect the sum of all polymeric forms (MTs, tubulin sheets and ribbons, and MT fragments) rather than uniform MTs only, as in the case of taxol and Epo B. Addition of MAPs (0.5 mg mL^{-1}) to free αβ-tubulin prior to polymerization did not markedly alter the architecture of polymers induced by DDM (Figure 2E).

Ultrasound (US) treatment of MSA-induced tubulin polymers

The observations described above raised the question of whether the short size and, in particular, the irregular nature of the DDM-induced polymers might affect the stability of these structures under conditions of physical stress. To test this hypothesis, physical stress was applied to fully grown MTs (GTP- or MSA-induced) by means of US. Intriguingly, even a 2 min high-frequency (40 kHz) US treatment of DDM-induced polymers led to a reduction in A_{340} by approximately 40%; this indicates that DDM-induced MTs and other polymerization products were partially destroyed under these conditions (Figure 4). In contrast, the polymerization curves observed with either taxol or Epo B were not affected by intermittent short-term exposure of the polymerization mixtures to US. Importantly, MTs assembled in the presence of GTP (0.5 mM) and monosodium glutamate (0.4 M) and in the absence of MSAs showed the same behavior as taxol- and Epo B-induced MTs and were found to be entirely stable to high-frequency US, as determined by turbidity measurements (data not shown).

The conclusions derived from the turbidimetry experiments are also supported by the results of EM studies. As illustrated by the electron micrographs shown in Figure 5, short-term (<5 min) US treatment resulted in both the disassembly of DDM-induced MTs as well as the agglutination of tubulin sheets and ribbons into clews. This is an important finding, as even significant changes in A_{340} might not always reflect large changes in the ratio of soluble to polymerized tubulin, and,

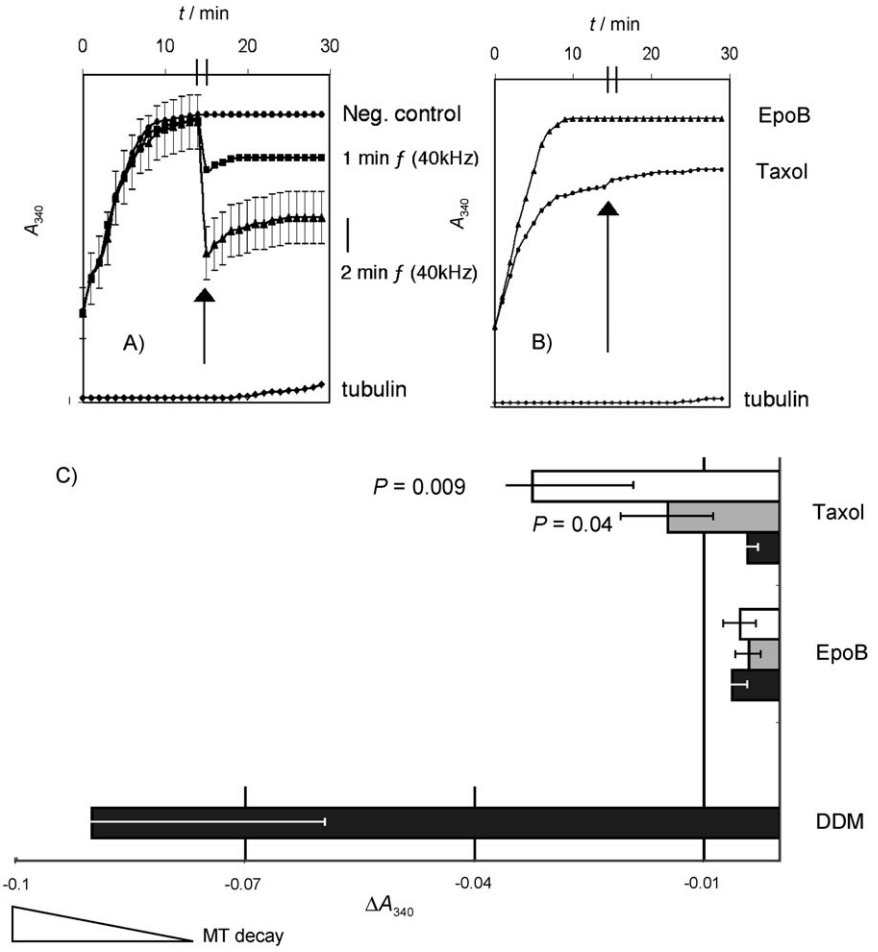

Figure 4. Turbidimetry-based assessment of the stability of MSA-induced tubulin polymers against US treatment (40 kHz, 1 min or 2 min, 22–25 °C). αβ-Tubulin (10 μM) was polymerized with an equimolar amount of the respective MSA in the absence of GTP. Depending on the experiment, different concentrations of DDM were employed. Arrows indicate time windows during which US treatment was applied. αβ-Tubulin negative controls are also shown. A) Short US exposure of active DDM-containing polymerization mixtures led to a significant decrease in A_{340}, thus indicating the degradation (disassembly) of polymerization products. B) Taxol- or Epo B-based MTs are not affected. C) DDM treatment of taxol-induced MTs leads to a concentration-dependent decrease in A_{340}. The graph shows the ΔA_{340} after the addition of DDM to MTs induced by taxol or Epo B and subsequent US treatment (2 min). Black bars: control (no DDM added); gray bars: 5 μM DDM added; white bars: 20 μM DDM added. The DDM bar shows the ΔA_{340} after a 2 min US exposure of DDM-induced MTs (corresponds to Figure 4A).

therefore, the extent of tubulin polymerization or disassembly, vide supra.

It should also be noted that the tubulin polymers obtained with DDM under our experimental conditions were completely resistant to cold-induced depolymerization (as deduced from turbidity measurements). This is in agreement with previously reported data for polymers obtained under different polymerization conditions,[14b] thus indicating that the polymers investigated here are not inherently less stable than those previously studied.

Given the distinct combination effects observed between DDM and taxol in cell growth inhibition experiments[14a] (vide supra), we also investigated the effect of DDM on the stability of taxol- or Epo B-induced MTs under physical stress conditions. The incubation of fully grown taxol-induced polymers (obtained from 10 μM tubulin and 10 μM taxol) with either 5 or 20 μM of DDM followed by a 2 min US exposure led to a measurable decrease in A_{340} (Figure 4C). The effect was concentration dependent, that is, it was more pronounced with 20 μM DDM (30% reduction in A_{340}) than with 5 μM DDM, and it strongly suggests that DDM reduces the stability of taxol-containing MTs under physical stress conditions. No change in A_{340} was observed upon the addition of a twofold molar excess of DDM (relative to MSA and tubulin) to Epo B-induced MTs (Figure 4C), which indicates that the stability of the latter is not affected by DDM. While we have not specifically investigated this question, the apparent destabilization of taxol-induced MTs by DDM may be a consequence of a (partial) displacement of taxol from its binding site, which could change the overall properties of the polymers to a more "DDM-like" state. The different effects of DDM on taxol- and Epo B-based MTs would then be a direct reflection of the much larger difference in MT-binding affinity between DDM and taxol (~400-fold) than for DDM and Epo B (~fourfold, in favor of DDM).[17]

In addition to the effects of DDM on taxol- and Epo B-containing preformed MTs, we also investigated the ability of taxol and Epo B to affect the state of the breakdown products derived from the US treatment of DDM-induced MTs. Thus, DDM-containing polymerization mixtures (polymerization period of 30 min) were subjected to a 2 min US treatment and then incubated with taxol or Epo B for 30 min at room temperature. Neither taxol nor Epo B, even when employed at a fivefold molar excess over tubulin, produced any increase in A_{340} (data not shown). This indicates that neither compound was able to induce reassembly of the breakdown products formed upon US treatment of DDM-induced MTs.

Combination studies

As indicated above, DDM and taxol, but not DDM and Epo B, exhibit pronounced synergism in the inhibition of human cancer cell growth in vitro.[14a] At the same time, the experi-

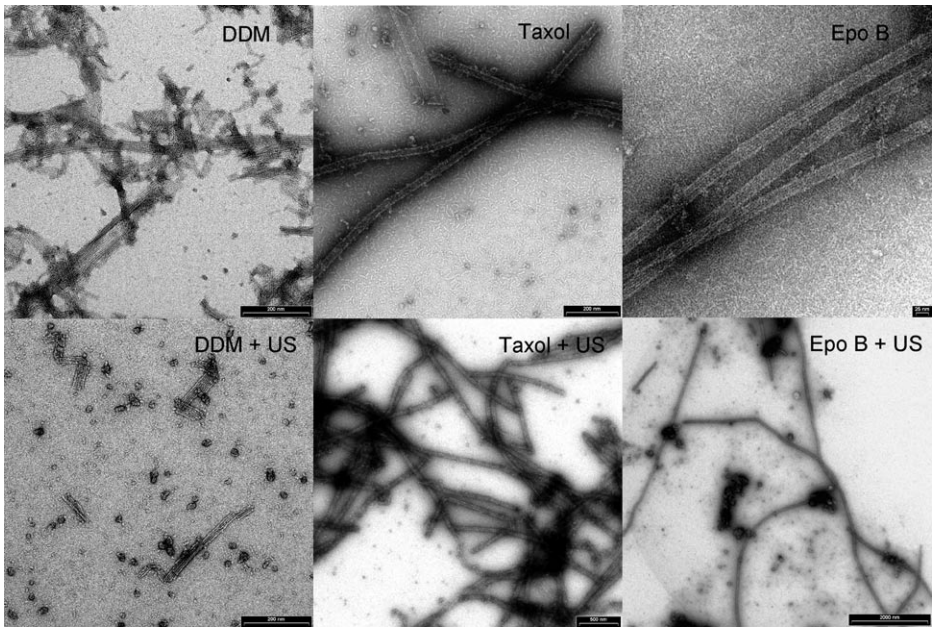

Figure 5. The effect of US on MSA-induced tubulin polymers. Upper row of micrographs: tubulin polymers induced by DDM, taxol, or Epo B (40 μM of drug/αβ-tubulin) prior to US treatment. Lower row of micrographs: corresponding preparations after a 2 min treatment with US (40 kHz). The size of the scale bars: DDM, Taxol, DDM + US: 200 nm; Epo B: 25 nm; Taxol + US: 500 nm; Epo B + US: 2000 nm.

ments discussed in the previous sections revealed distinctly different effects of DDM, compared with that of either taxol or Epo B, on tubulin polymerization kinetics, polymer morphology, and the stability of polymerization products. Collectively, these findings raised the question about the effects of DDM/taxol and DDM/Epo B combinations on tubulin polymerization and the nature of the polymers that would be formed in this process. Thus, we investigated the induction of tubulin polymerization by equimolar mixtures of DDM/taxol, DDM/Epo B, and taxol/Epo B. These experiments were performed in the presence of MAPs and free αβ-tubulin in excess (1 equiv of each MSA, 3 equiv tubulin), in order to provide a sufficient number of binding sites for the complete binding of both MSAs.

The centrifugation-based T_{max} observed upon simultaneous incubation of tubulin/MAPs with DDM and taxol, (387 ± 131) s, was comparable with that obtained for DDM alone, (420 ± 139) s, and thus, was significantly lower than the T_{max} for taxol ((1024 ± 177) s; Figure 6). In contrast, combinations of DDM and Epo B or taxol and Epo B produced T_{max} values that roughly corresponded with the higher of the T_{max} values of the individual combination partners (Epo B in both cases; DDM/Epo B: T_{max} = (1565 ± 218) min; Epo B/taxol: T_{max} = (1484 ± 275) min; Figure 6).

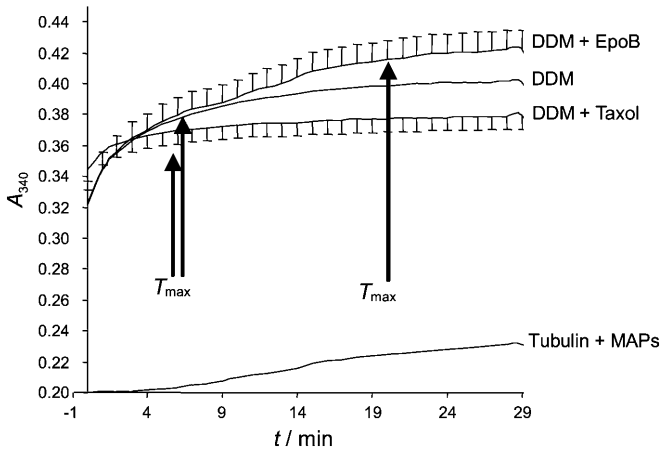

Figure 6. Tubulin polymerization induced by equimolar mixtures of DDM and taxol or of DDM and Epo B. Each MSA (10 μM) was added simultaneously to αβ-tubulin (30 μM)/MAPs (0.5 mg mL^{-1}). Data points are average values from three experiments ± SEM. Arrows indicate T_{max} as determined by the centrifugation method.

At the same time, and quite intriguingly, the architecture of the DDM/taxol-induced MTs appeared to be intermediate between that of the MTs formed with either of the two agents alone (Figure 7). The DDM/taxol-induced MTs tended to be shorter (1–3 μm) than those induced by taxol (1–10 μm), but longer than the polymers formed with DDM (~1 μm). Significantly, the characteristic tubulin sheets observed with DDM alone were almost completely absent from polymer preparations obtained with the DDM/taxol combination (Figure 7).

A more detailed analysis of the DDM/taxol-induced polymeric structures revealed the presence of randomly distributed areas across the polymer where the cylinder was opened and distorted; these might represent accumulation sites of DDM (Figure 7). At the same time, only few broken fragments were visible. Internal distortions of the MT cylinder were virtually absent from MTs assembled with taxol alone (under identical conditions), although they may occur close to MT ends (data not shown).

The EM analysis of DDM/Epo B-induced polymers was inconclusive, but seemed to indicate the formation of two independent types of MTs (corresponding to those in Figure 1; data for combination experiments not shown). This would be in line with the results of the T_{max} measurements, as the T_{max} for the combination in this case would be expected to correspond to the higher of the T_{max} values for the two combination partners (i.e., Epo B). However, at this point in time, these assumptions are purely speculative, and additional experiments will be required to either confirm or reject the hypothesis of independent polymer formation for mixtures of DDM and Epo B.

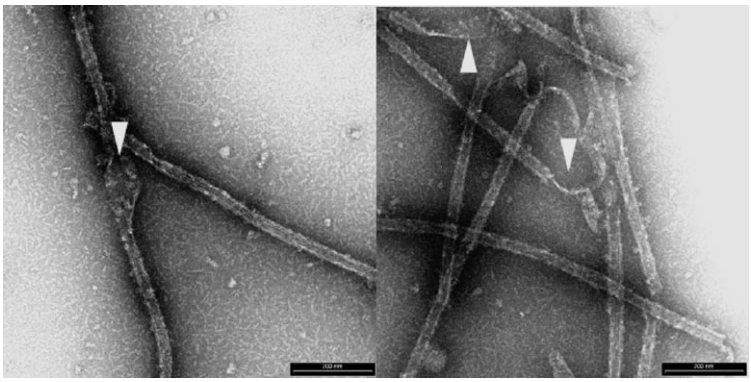

Figure 7. Electron micrographs of MTs formed with equimolar amounts of DDM and taxol. DDM (13.3 μM) and taxol (13.3 μM) were simultaneously incubated with αβ-tubulin (40 μM)/MAPs (0.5 mg mL^{-1}). White arrows indicate regions displaying structural features of DDM-induced MTs (Figure 2). The scale bars are 200 nm.

Surprisingly, the US treatment of MTs formed with the DDM/taxol combination revealed that they had apparently lost the hyperfragile character of the DDM-induced polymers (data not shown). This seems to contradict the previous observation of the destabilizing effect of DDM on taxol-induced preformed MTs. The reasons for this discrepancy have not been specifically addressed, but could perhaps be related to differences in β-tubulin isotype composition and distribution between the MTs assembled with either taxol alone or a taxol/DDM mixture (vide infra).

β-Tubulin isotype composition of MSA-assembled MTs

Previous studies have demonstrated that the dynamicity and stability of MTs strongly depend on their isotype composition. For example, it has been known for some time that MTs assembled, in vitro, solely from $\alpha\beta_{III}$ dimers exhibit distinct assembly properties[27] and significantly enhanced dynamics relative to MTs derived from either $\alpha\beta_{II}$ or $\alpha\beta_{IV}$ dimers or from unfractionated tubulin.[28] These experimental findings were extended in a recent study by Rezania et al., and the collective data were analyzed by using an approach based on recursive maps.[29] As a result, these authors suggested that the interactions between dimers of different isotypes during polymer growth are stronger than those between dimers of the same isotype. For example, the incorporation of new $\alpha\beta_{II}$ dimers during MT polymerization is predicted to occur preferentially next to an $\alpha\beta_{III}$ rather than an $\alpha\beta_{II}$ dimer, and vice versa.[29] As a consequence, MTs assembled from mixtures of different tubulin isotypes should be less dynamic (more stable) than those formed with one isotype only, which is what is experimentally observed.

Based on this model, the differences in morphology and stability observed in our study between MTs assembled with DDM and taxol or Epo B could be related to differences in αβ-tubulin isotype usage by different MSAs in the course of the polymerization process. In order to address this question, we analyzed the $\alpha\beta_{I/II}$- and $\alpha\beta_{III}$-dimer content of the MTs induced by DDM, taxol, or Epo B from purified (mixed isotype) αβ-tubulin in the absence of GTP by means of Western blotting.

Initial experiments were conducted with equimolar amounts of αβ-tubulin and MSAs, but no significant differences were observed between the Western blots of polymerization mixtures obtained with the different MSAs under these conditions. However, when αβ-tubulin was employed in a fivefold molar excess over the inducing agent, the fraction of $\alpha\beta_{III}$ dimers was markedly lower in DDM-induced MTs than in those obtained with either taxol or Epo B (Figure 8). This finding strongly suggests that DDM has a pattern of isotype usage during tubulin polymerization that is different from that of taxol and Epo B, and is characterized by a lower affinity for $\alpha\beta_{III}$-tubulin. Under conditions where αβ-tubulin and DDM are present in a 1:1 ratio, this may become manifest in the incorporation of $\alpha\beta_{III}$-type dimers only towards the end of the polymerization process. As a consequence, the isotype composition for the bulk of the MTs would be more homogeneous; this results in more dynamic, less stable MTs (vide supra).

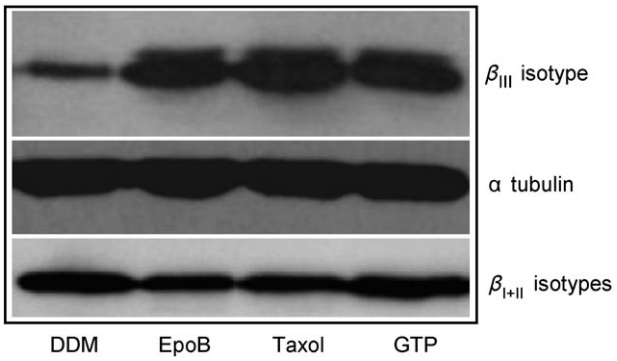

Figure 8. Western blots of tubulin polymers obtained with MSAs (10 μM) and purified pig brain tubulin (50 μM) in the absence of GTP (1 h incubation at room temperature). Control MTs were assembled with GTP (25 mM) and glutamate (2.7 M). Monoclonal antibodies were used for immunostaining of the β-tubulin isotypes.

The above differences in isotype usage between DDM and taxol also suggest that MTs assembled with a DDM/taxol mixture and those obtained with taxol alone might differ in their isotype composition and distribution (across the MT). This could provide a rationale for the US resistance of MTs formed with DDM/taxol, while taxol-induced MTs become less stable to US treatment in the presence of added DDM.

Conclusions

The experiments performed in this study demonstrated that DDM induces the formation of MT polymers, whose architecture was clearly distinguishable from that of taxol- or Epo B-induced structures. While these findings partly reconfirm previous literature reports,[18] we were also able to show that the differences in morphology between DDM-induced MTs and those obtained with either taxol or Epo B translate into distinct differences in physicochemical properties. Thus, DDM-induced

MT polymers can be destroyed by US treatment, whereas those formed with taxol or Epo B are stable. While the biological significance of these findings is unknown, they still highlight the existence of fundamental differences in the physicochemical properties between DDM- and taxol- or Epo B-induced tubulin polymers, which could also be relevant at the biological level.

DDM-induced MT assembly was found to be distinct from taxol- or Epo B-driven polymerization not only at the level of polymer morphology and stability but also regarding the usage of different tubulin isotypes. Thus, under conditions in which MSA availability is limiting, DDM-induced MTs contained significantly less $\alpha\beta_{III}$-tubulin than those assembled with either taxol or Epo B. While no such difference could be detected (within the accuracy limits of Western blot analysis) when MSAs and $\alpha\beta$-tubulin were present in a 1:1 ratio, the less efficient usage of $\alpha\beta_{III}$-tubulin by DDM could lead to changes in polymer stability due to changes in the intramicrotubular distribution of tubulin isotypes. Clearly, a more comprehensive understanding of the differential effects of MSAs on tubulin polymerization and MT stability will require a detailed assessment of tubulin isotype usage by these agents during the polymerization process.

Subtle but significant differences between DDM and taxol have been reported for cellular systems. Thus, DDM has been shown to produce shorter MTs and to induce strong MT bundling in cells[18a,30] and, in comparison to taxol, exhibit stronger MT-stabilizing effects.[18a,30] On the other hand, the concentrations required to produce mitotic arrest by DDM appear to be significantly higher than those required to inhibit human cancer cell proliferation,[16,31] and we have confirmed this phenomenon in our own laboratory (B. Sager, J.G., unpublished data). More recently, DDM was also found to induce accelerated senescence in A549 cells, whereas taxol did not.[32] Based on our experiments, it is not inconceivable that these effects are due to differences in MT architecture between DDM- and taxol-induced MTs rather than being related to interactions (of DDM) with additional protein targets. Cell-based experiments in our own laboratory have also shown that incubation of MonoMac-6 cells with high concentrations of DDM (1 μM) over short time periods leads to the extensive formation of bundles, which are rapidly transported into pseudopodia, thereby inducing a distinct cellular morphology (J.G., unpublished data). Similar effects have previously been observed with mouse fibroblasts,[30] and no such changes in cellular morphology were induced in MonoMac-6 cells with either taxol or Epo B. Based on immunofluorescence staining, the DDM-induced bundles in MonoMac-6 cells appear to be largely composed of shorter MTs (in comparison to taxol- or Epo B-induced bundles) and/or $\alpha\beta$-tubulin sheets that assemble laterally and cluster without forming a tube.

Finally, our study points to the formation of a new type of MT polymer with a mixed morphology in the simultaneous presence of DDM and taxol. These findings parallel the previously reported cellular synergism between DDM and taxol.[14a] Future studies will show whether our findings with isolated tubulin are of relevance for cellular systems, and whether MT architecture could become a relevant aspect in MT-based drug discovery.

Experimental Section

Chemicals: (+)-DDM and Epo B were generous gifts of the Novartis Pharmaceuticals Corp. (Basel, Switzerland); taxol (paclitaxel) was purchased from Sigma. Compounds were used as stock solutions (2 mM) in DMSO. DMSO, GTP, ATP, PIPES, and EGTA were obtained from Fluka. Monoclonal antibodies against β-tubulin isotypes and a polyclonal antibody against α-tubulin were purchased from Abcam (Ab11314, Ab11313, Ab151246) and employed according to the manufacturer's instructions.

Isolation of pure αβ-tubulin (>95%): Tubulin was isolated as pure $\alpha\beta$-tubulin from fresh pig brain tissue according to the method of Castoldi and Popov.[33] Fresh brain tissue was obtained from a local slaughterhouse and processed immediately without prior cooling. In brief, cleaned pig brain tissue (150–200 g) was put into ice-cold depolymerization buffer (50 mM MES, 1 mM $CaCl_2$, adjusted to pH 6.9 with KOH) and homogenized in a Polytron mixer. The homogenate was centrifuged in a Sorvall SLA-1500 rotor at 14500 rpm for 60 min. The supernatant was transferred into an Erlenmeyer flask in high-molarity PIPES buffer (1 M PIPES, 10 mM $MgCl_2$, 20 mM EGTA adjusted to pH 6.9 with KOH) plus ATP (1.5 mM final concentration) and glycerol (98%) in a total volume of 300 mL. The resulting suspension was mixed and incubated at 37 °C for 1 h. Aliquots were transferred into ultracentrifuge tubes and centrifuged in a Beckman Ti50.2 rotor at 32500 rpm (96000 *g*) for 75 min at 30 °C. The MT protein pellets were resuspended in depolymerization buffer and put on ice prior to ultracentrifugation at 4 °C. The procedure was repeated for two polymerization cycles (total of three cycles), and the final $\alpha\beta$-tubulin pellets were dissolved in ice-cold Brinkley Buffer (BRB80: 80 mM PIPES, 1 mM $MgCl_2$, 1 mM EGTA adjusted to pH 6.8 with KOH) prior to shock-freezing in liquid N_2 and subsequent storage at −80 °C. The $\alpha\beta$-tubulin purity and concentration were determined by SDS-PAGE gel electrophoresis and spectrophotometrically ($A = \varepsilon \times c \times d$ with an extinction coefficient of 115000 $M^{-1}cm^{-1}$ at 280 nm). This procedure typically yielded 60–100 mg of $\alpha\beta$-tubulin per 100 g of brain tissue with a purity >95%. Notably, this method of tubulin preparation results in tubulin with GDP in the exchangeable site with only traces of GTP. No GTP, MAPs, or glutamate was used in polymerization experiments with this tubulin unless specifically stated.

Preparation of MAPs: Heat-treated MAPs were prepared from fresh pig brain tissue according to a method previously published by Hamel et al.[23] The MAPs preparation was lyophilized and stored at −80 °C. The purity and concentration were determined by SDS-PAGE gel electrophoresis. In experiments employing MAPs, 0.5 mg mL^{-1} were added to $\alpha\beta$-tubulin preparations.

Electron microscopy (EM): Conventional transmission EM (both bright- and dark-field) was performed at the Electron Microscopy Center, EMEZ ETH, Zürich. MT samples were prepared in BRB80 buffer, in general, with stoichiometric amounts of drug/$\alpha\beta$-tubulin. Samples (5 μL) of MT from preparations were loaded onto a freshly prepared copper grid. The grid was blotted dry with filter paper 15–20 s later, and the MT preparations were stained with uranyl acetate (2%) for 20 s. For negative staining, an aliquot (5 μL) of the sample was adsorbed for 60 s onto glow-discharged carbon-coated collodium film on a 400 mesh per inch copper grid. The grid was next washed with two drops of distilled water, stained for 20 s with uranyl formate (0.75%, pH 4.25), and air dried after the

removal of excess liquid with filter paper and suction with a capillary applied to the edge of the grid. Specimens were examined in a Hitachi H-8000 TEM (Hitachi, Ltd.), operated at 100 kV. The numbers of MTs were counted from prints of different grid areas (176 μm^2 each). Polymers were chosen randomly for analysis.

Tubulin polymerization: Freshly thawed αβ-tubulin was centrifuged at 5000 *g* for 5 min at 5 °C and then incubated with additional BRB80 buffer, MSAs, DMSO vehicle (2%), GTP/glutamate (0.5 mM/0.4 M final concentration if not stated otherwise), and/or MAPs (0.5 mg mL^{-1}) in a 96-well plate in either 50 or 100 μL volumes. MSA-driven polymerization was investigated in the absence of GTP. Compounds were added to the tubulin solution on ice. Experiments were either carried out in a 96-well quartz plate or in normal 96-well polystyrene plates (Falcon). The polymerization was monitored by following the increase in absorption at 340 nm in a temperature-controlled TECAN GeniosPro spectrophotometer. Depending on the specific experiment, the temperature was set either to room temperature (actual measuring temperature was 24–27 °C) or 37 °C. The concentration of DMSO was found to be highly critical, as DMSO concentrations $>2\%$ induced considerable MT formation. All experiments, including both negative (untreated αβ-tubulin) and vehicle controls, were carried out in triplicate. Experiments were performed with at least two different αβ-tubulin batches. Average differences in A340 were subjected to statistical analysis (student *t*-test and ANOVA), and $P<0.05$ was considered to be significant.

Determination of the time required to achieve maximum polymerization (T_{max}). Several drug/αβ-tubulin mixtures were run in parallel in these experiments. After an initial polymerization time of 120 s for all samples, individual mixtures were removed every minute and centrifuged. The remaining amount of unpolymerized αβ-tubulin in these samples was determined according to Lin et al.,[24] that is, employing a standard Bradford method (Pierce Biotechnology). T_{max} was determined from a curve generated with the Graphpad Prism 4 software (A_{340} in the presence of MSA alone/A_{340} for MSA + GTP) and defined as the time point at which the quantifiable amount of tubulin in the supernatant did not decrease further. This method was also employed to determine the maximum degree of conversion of tubulin into MT polymers (% polymerization) induced by each MSA. In an alternative approach, the absorption of the polymerization mixtures was followed at 340 nm and assumed to be proportional to the amount of MT polymer formed.[23] After the MSA addition, glutamate (2.7 M) and GTP (25 mM) were added to the polymerization mixture every minute to assess whether free αβ-tubulin (or oligomers not associated with MTs) was still present. This was judged by the appearance and height of a second polymerization curve (a further increase in A_{340}), which was assumed to indicate the presence of remaining free αβ-tubulin or oligomers not detectable at 340 nm. In this method, T_{max} was determined from a curve generated with the Graphpad Prism 4 software and defined as the time point at which no second polymerization curve could be detected upon the addition of glutamate/GTP.

Ultrasound (US) treatment of polymers: Polystyrene 96-well plates containing the samples from the polymerization assays were carefully sealed with parafilm. A Merck ASB 40 kHz US water bath was filled with deionized water (10 cm deep), and the 96-well plates were carefully placed on the surface to float. Sonication was performed for different time periods. After sonication, the plate was carefully dried and left for 10 min on a shaking table. This latter incubation step was crucial to obtain reproducible results.

Keywords: discodermolide · microtubule stabilizer · microtubules · natural products · proteins

[1] For recent reviews on microtubule-stabilizing agents, see: a) K.-H. Altmann, J. Gertsch, *Nat. Prod. Rep.* **2007**, *24*, 327–357; b) D. C. Myles, *Annu. Rep. Med. Chem.* **2002**, *37*, 125–132; c) K.-H. Altmann, *Curr. Opin. Chem. Biol.* **2001**, *5*, 424–431.
[2] For reviews on MT structure and function, see: a) M. A. Jordan, L. Wilson, *Nat. Rev. Cancer* **2004**, *4*, 253–265; b) E. Nogales, *Annu. Rev. Biophys. Biomol. Struct.* **2001**, *30*, 397–420; c) O. Valiron, N. Caudron, D. Job, *Cell. Mol. Life Sci.* **2001**, *58*, 2069–2084; d) L. Amos, *Org. Biomol. Chem.* **2004**, *2*, 2153–2160.
[3] M. A. Jordan, *Curr. Med. Chem: Anti-Cancer Agents* **2002**, *2*, 1–14.
[4] a) Y. Zhai, P. J. Kronebusch, P. M. Simon, G. G. Borisy, *J. Cell Biol.* **1996**, *135*, 201–214; b) N. M. Rusan, C. J. Fagerstrom, A.-M. C. Yvon, P. Wadsworth, *Mol. Biol. Cell* **2001**, *12*, 971–980.
[5] a) J. Crown, M. O'Leary, W.-S. Ooi, *Oncologist* **2004**, *9 (Suppl. 2)*, 24–32; b) E. K. Rowinsky, *Annu. Rev. Med.* **1997**, *48*, 353–374.
[6] M. C. Wani, H. L. Taylor, M. E. Wall, P. Coggon, A. T. McPhail, *J. Am. Chem. Soc.* **1971**, *93*, 2325–2327.
[7] P. B. Schiff, J. Fant, S. B. Horwitz, *Nature* **1979**, *277*, 665–667.
[8] For recent reviews on epothilones, see: a) K.-H. Altmann, B. Pfeiffer, S. Arseniyadis, B. A. Pratt, K. C. Nicolaou, *ChemMedChem* **2007**, *2*, 396–423; b) G. Höfle, H. Reichenbach in *Anticancer Agents from Natural Products* (Eds.: G. M. Cragg, D. G. I. Kingston, D. J. Newman), CRC Press, Boca Raton, **2005**, pp. 413–450.
[9] For recent reviews on clinical trials with Epo B (EPO906, patupilone), see: a) M. Harrison, C. Swanton, *Exp Opin. Investig. Drugs* **2008**, *17*, 523–546; b) J. M. G. Larkin, S. B. Kaye, *Expert Opin. Invest. Drugs* **2006**, *15*, 691–702.
[10] According to company information, clinical trials with DDM were terminated by Novartis after phase I.
[11] http://www.novartisoncology.com/page/patupilone.jsp.
[12] Ixabepilone is marketed in the US by Bristol–Myers Squibb (BMS) under the trade name Ixempra®: E. Kaminskas, X. Jiang, R. Aziz, J. Bullock, R. Kasliwal, R. Harapanhalli, S. Pope, R. Sridhara, J. Leighton, B. Booth, R. Dagher, R. Justice, R. Pazdur, *Clin. Cancer Res.* **2008**, *14*, 4378–4384. For leading references on ixabepilone, see: a) E. S. Thomas, H. L. Gomez, R. K. Li, H.-C. Chung, L. E. Fein, V. F. Chan, J. Jassem, X. B. Pivot, J. Klimovsky, F. Hurtado de Mendoza, B. Xu, M. Campone, G. L. Lerzo, R. A. Peck, P. Mukhopadhyay, L. T. Vahdat, H. H. Roche, *J. Clin. Oncol.* **2007**, *25*, 5210–5217; b) F. Y. F. Lee, R. Borzilleri, C. R. Fairchild, S. H. Kim, B. H. Long, C. Reventos-Suarez, G. D. Vite, W. C. Rose, R. A. Kramer, *Clin. Cancer Res.* **2001**, *7*, 1429–1437; c) R. M. Borzilleri, X. P. Zheng, R. J. Schmidt, J. A. Johnson, S. H. Kim, J. D. DiMarco, C. R. Fairchild, J. Z. Gougoutas, F. Y. F. Lee, B. H. Long, G. D. Vite, *J. Am. Chem. Soc.* **2000**, *122*, 8890–8897.
[13] a) K.-H. Altmann, M. Wartmann, T. O'Reilly, *Biochim. Biophys. Acta Rev. Cancer* **2000**, *1470*, M79–M91; b) R. J. Kowalski, P. Giannakakou, E. Hamel, *J. Biol. Chem.* **1997**, *272*, 2534–2541; c) D. M. Bollag, P. A. McQueney, J. Zhu, O. Hensens, L. Koupal, J. Liesch, M. Goetz, E. Lazarides, C. M. Woods, *Cancer Res.* **1995**, *55*, 2325–2333.
[14] a) L. A. Martello, H. M. McDaid, D. L. Regl, C. P. H. Yang, D. Meng, T. R. R. Pettus, M. D. Kaufman, H. Arimoto, S. J. Danishefsky, A. B. Smith III, S. B. Horwitz, *Clin. Cancer Res.* **2000**, *6*, 1978–1987; b) E. ter Haar, R. J. Kowalski, E. Hamel, C. M. Lin, R. E. Longley, S. P. Gunasekara, H. S. Rosenkranz, B. W. Day, *Biochemistry* **1996**, *35*, 243–250.
[15] G. S. Huang, L. Lopez-Barcons, B. S. Freeze, A. B. Smith III, G. L. Goldberg, S. B. Horwitz, H. M. McDaid, *Clin. Cancer Res.* **2006**, *12*, 298–304.
[16] S. Honore, K. Kamath, D. Braguer, L. Wilson, C. Briand, M. A. Jordan, *Mol. Cancer Ther.* **2003**, *2*, 1303–1311.
[17] R. M. Buey, I. Barasoain, E. Jackson, A. Meyer, P. Giannakakou, I. Paterson, S. Mooberry, J. M. Andreu, J. F. Diaz, *Chem. Biol.* **2005**, *12*, 1269–1279.
[18] a) L. A. Martello, M. J. LaMarche, L. He, T. J. Beauchamp, A. B. Smith III, S. B. Horwitz, *Chem. Biol.* **2001**, *8*, 843–855; b) R. J. Kowalski, P. Giannakakou, S. P. Gunasekera, R. E. Longley, B. W. Day, E. Hamel, *Mol. Pharmacol.* **1997**, *52*, 613–622.
[19] P. Meurer-Grob, J. Kasparian, R. H. Wade, *Biochemistry* **2001**, *40*, 8000–8008.

[20] E. J. Gapud, R. Bai, A. K. Ghosh, E. Hamel, *Mol. Pharmacol.* **2004**, *66*, 113–121.
[21] D. E. Pryor, A. O'Brate, G. Bilcer, J. F. Diaz, Y. Wang, Y. Wang, M. Kabaki, M. K. Jung, J. M. Andreu, A. K. Ghosh, P. Giannakakou, E. Hamel, *Biochemistry* **2002**, *41*, 9109–9115.
[22] Combinations of laulimalide or peloruside A (neither of which binds to the taxoid site on β-tubulin) with taxoid-site MSAs were recently evaluated for their effects on tubulin polymerization but not on MT morphology: a) A. Wilmes, K. Bargh, C. Kelly, P. T. Northcote, J. H. Miller, *Mol. Pharm.* **2007**, *4*, 269–280; b) E. Hamel, B. W. Day, J. H. Miller, M. K. Jung, P. T. Northcote, A. K. Ghosh, D. P. Curran, M. Cushman, K. C. Nicolaou, I. Paterson, E. J. Sorensen, *Mol. Pharmacol.* **2006**, *70*, 1555–1564.
[23] E. Hamel, A. A. del Campo, J. Lustbader, C. M. Lin, *Biochemistry* **1983**, *22*, 1271–1279.
[24] C. M. Lin, Y. Q. Jiang, A. G. Chaudhary, J. M. Rimoldi, D. G. I. Kingston, E. Hamel, *Cancer Chemother. Pharmacol.* **1996**, *38*, 136–140.
[25] D. T. Hung, J. Chen, S. L. Schreiber, *Chem. Biol.* **1996**, *3*, 287–293.
[26] D. A. Dabydeen, G. J. Florence, I. Paterson, E. Hamel, *Cancer Chemother. Pharmacol.* **2004**, *53*, 397–403.
[27] a) Q. Lu, R. F. Luduena, *J. Biol. Chem.* **1994**, *269*, 2041–2047; b) Q. Lu, R. F. Luduena, *Cell Struct. Funct.* **1993**, *18*, 173–182; c) A. Banerjee, M. C. Roach, P. Trcka, R. F. Luduena, *J. Biol. Chem.* **1990**, *265*, 1794–1799.
[28] D. Panda, H. P. Miller, A. Banerjee, R. F. Luduena, L. Wilson, *Proc. Natl. Acad. Sci. USA* **1994**, *91*, 11358–11362.
[29] V. Rezania, O. Azarenko, M. A. Jordan, H. Bolterauer, R. F. Luduena, J. T. Huzil, J. A. Tuszynski, *Biophys. J.* **2008**, *95*, 1993–2008.
[30] F. Sasse, *Curr. Biol.* **2000**, *10*, R469.
[31] C. Madiraju, M. C. Edler, E. Hamel, B. S. Raccor, S. Brianne, R. Van Balachandran, G. Zhu, K. A. Giuliano, A. Vogt, Y. Shin, J.-H. Fournier, Y. Fukui, A. M. Brückner, D. P. Curran, B. W. Day, *Biochemistry* **2005**, *44*, 15053–15063.
[32] L. E. Klein, B. S. Freeze, A. B. Smith III, S. B. Horwitz, *Cell Cycle* **2005**, *4*, 501–507.
[33] M. Castoldi, A. V. Popov, *Protein Expression Purif.* **2003**, *32*, 83–88.

Received: August 19, 2008
Published online on December 4, 2008

